Sensors and Actuators B 207 (2015) 581–587

Contents lists available at ScienceDirect

Sensors and Actuators B: Chemical

journal homepage: www.elsevier.com/locate/snb

How low does the oxygen concentration go within a sandwich-type amperometric biosensor? Part 2: Theory for PPO biosensors

Fernando Garay*

INFIQC – CONICET, Dpto. de Físico Química, Facultad de Ciencias Químicas, UNC, Pab. Argentina, ala 1, 2° piso, Ciudad Universitaria, 5000 Córdoba, Argentina

ARTICLE INFO

Article history:
Received 9 June 2014
Received in revised form 4 October 2014
Accepted 23 October 2014
Available online 1 November 2014

Keywords:
Ping-pong
PPO
Sandwich-type biosensor
Polyphenol oxidase
Amperometric sensor
Mathematical modeling

ABSTRACT

A mathematical model to describe the amperometric response of a sandwich-type biosensor containing polyphenol oxidase as the recognition catalytic element is proposed. The model was solved numerically and the resulting nonlinear solution was used to simulate chronoamperometric curves as well as to estimate the concentration profiles of reagents and products of the enzymatic reaction within the sensor. Fromm's systematic method was applied to get a kinetic expression for the analysis of polyphenol oxidase enzymes. The simulated data are compared with curves corresponding to a biosensor prepared with an oxidase enzyme that reacts according to a ping-pong mechanism. Although in both cases oxygen is used as mediator of the enzymatic reaction, the electrochemical step can generate it back from the H_2O_2 released by enzymes such as glucose oxidase but it cannot do the same in the case of working with polyphenol oxidase. Most of the calculated profiles and related data are presented using dimensioned variables so that they can be directly compared with experimental results. Relevant parameters such as limit current, response-time, and sensitivity are analyzed as function of the thickness of membranes, concentration of enzyme and concentration of substrate.

1. Introduction

The high specificity of enzymes enabled the development of biosensors, which are devices that can recognize specific substrates in samples with very complex matrixes [1–4]. The enzymatic reaction is typically detected by electrochemical or spectroscopic transducers [4–9]. A widely used detection strategy corresponds to the amperometric biosensors that use an oxidoreductase enzyme for changing the oxidation state of the substrate [1,4,6]. Recently we have developed a model to describe the concentration of reagents and products within a sandwich-type amperometric biosensor in which the following reactions take place [10,11]:

$$E_r + S \underset{k_{-1}}{\overset{k_1}{\rightleftarrows}} E_rS \xrightarrow{k_2} E_o + R \quad (1)$$

$$E_o + M \underset{k_{-3}}{\overset{k_3}{\rightleftarrows}} E_oM \xrightarrow{k_4} E_r + Q \quad (2)$$

Those reactions correspond to a ping-pong reaction mechanism that will be referred as system 1 in this manuscript. It is considered that the sensor corresponds to a first generation biosensor where E_r and E_o are the reduced and oxidized forms of the enzyme and where E_rS and E_oM are the intermediate complexes of the enzyme with substrate (S) and mediator (M), respectively [10]. The equations proposed to describe a ping-pong reaction mechanism have been summarized in Appendix A and further details can be found elsewhere [10,11].

The reaction mechanism of a polyphenol oxidase (PPO) has a more complicated reaction mechanism where oxygen, the natural mediator of this enzyme, is transformed into water and two molecules of a diphenol are consumed per enzymatic cycle [12]. In this case, O_2 cannot be easily replaced by other redox mediators and in some cases it might limit the enzymatic reaction. In this regard, it has to be considered that a value of $C_M = 0.274$ mM corresponds to the saturated oxygen concentration in blood and so, this would be the maximum value that can be assumed for this kind of system [13]. Although it is very difficult to measure the concentration profile of O_2 into the enzymatic matrix of a biosensor where the concentration can vary dramatically within few micrometers, it is still possible to calculate and estimate the concentration changes of involved species within a biosensor [10,11,14,15]. Those results would help us to optimize the performance of a PPO biosensor as

* Tel.: +54 351 5353866x53541; fax: +54 351 4334188.
E-mail addresses: fsgaray@gmail.com, fgaray@fcq.unc.edu.ar

http://dx.doi.org/10.1016/j.snb.2014.10.105
0925-4005/

well as to explain why a given calibration curve provides better or worse result than other [16–19].

The aim of this work is to develop a model that simulates chronoamperometric and concentration profiles corresponding to a PPO sandwich-type amperometric biosensor. The enzymatic reaction of PPO will be referred as system 2. The idea is to compare the reaction mechanism of enzymes such as glucose oxidase (GOX) and PPO to show their major differences, and to remark that none of those systems can be properly described by employing the Michaelis–Menten equation [10,11,15,20–22]. To do this, chronoamperometric responses and concentration profiles of sandwich-type biosensors involving enzymes associated with system 1 or 2 are compared. In order to evaluate the dynamic response of these nonlinear systems, numerical solutions are employed. The results can be used to estimate the concentration of reagents and products within a PPO biosensor and to determine the experimental parameters that would optimize the analytical response of this kind of devices [11].

2. The model

The reaction mechanism of a PPO involves a quite complex linear system that can be summarized as follow:

$$E_r + M \underset{k_2}{\overset{k_1}{\rightleftarrows}} E_o P_2 \tag{3}$$

Eq. (3) shows a first step where, the reduced form of the enzyme (E_r) is oxidized to (E_o) by the mediator O_2 [12]. Reactions such as:

$$E_r M \underset{k_{j+1}}{\overset{k_j}{\rightleftarrows}} E_o P_2 \tag{4}$$

are omitted, because steady-state is assumed for these steps [23]. Therefore, the treatment is insensitive to internal intermediates of this kind [23]. After the oxidation step, the reaction mechanism can be abbreviated as:

$$E_o P_2 + S \underset{k_4}{\overset{k_3}{\rightleftarrows}} E_o P_2 Q \underset{k_6}{\overset{k_5}{\rightleftarrows}} E_o P_2 + Q \tag{5}$$

$$E_o P_2 \underset{k_8}{\overset{k_7}{\rightleftarrows}} E_m P + P \tag{6}$$

$$E_m P + S \underset{k_{10}}{\overset{k_9}{\rightleftarrows}} E_r P Q \underset{k_{12}}{\overset{k_{11}}{\rightleftarrows}} E_r + P + Q \tag{7}$$

where E_m is an intermediate redox form of the enzyme, while the products Q and P correspond in this case to quinone and water, respectively. Other species are intermediate complexes of PPO with the involved substrates and/or products. Eqs. (3) and (5)–(7) describe the system 2. In this work Eqs. (3) and (5)–(7) have been evaluated according to the Fromm's systematic method to get the respective steady-state rate expression [23]. After applying this procedure, it was obtained the following expression for the velocity of the enzymatic reaction:

$$v = \frac{v_{max}}{1 + (K_S/C_S) + (K_M/C_M) + (K_{SM}/C_S C_M)} \tag{8}$$

where $K_S = [k_7 k_9 k_{11}(k_4 + k_5) + k_3 k_5 (k_7 + k_8)(k_{10} + k_{11})](k_3 k_9 k_v)^{-1}$, $v_{max} = 2\, C_E k_5 k_7 k_{11} (k_v)^{-1} = C_E k_{cat}$, $K_M = k_5 k_7 k_{11} (k_1 k_v)^{-1}$, $K_{SM} = k_2 k_7 k_{11}(k_4 + k_5)(k_1 k_3 k_v)^{-1}$, and $k_v = k_5 k_{11} + k_7 k_{11} + k_5 k_7$. The constants K_S, K_M, and K_{SM} are usually called Michaelis' constants, C_E is the total concentration of the enzyme within the sensor, and the variables C_M and C_S indicate the concentrations for M and S, respectively. All calculations have been performed assuming that $C_M^* = 0.274$ mM, which is the saturated oxygen concentration in blood [13].

At the electrode surface, the reduction of quinones to phenols takes place according to:

$$Q \underset{2H^+}{\overset{2e^-}{\rightleftarrows}} S \tag{9}$$

The boundary conditions of this model are related to a sandwich-type amperometric biosensor, in which the enzyme is confined within a matrix such as that of the scheme of Fig. 1. It is considered that, before the addition of the substrate, the concentrations of E_r and oxygen are constants and the values of C_S and C_Q are equal to zero. The electrode potential is selected to rapidly reduce Q to S. The stoichiometric relationship between the enzymatic reaction and the electrochemical process is considered by $v = n_i v_i$, where n_i corresponds to the stoichiometric coefficient of i species in the global enzymatic reaction [12]. Effects such as diffusion of protons and migration of charged species are neglected [24,25].

It is assumed that there is linear mass transfer along the x-axis, which is normal to the electrode surface [10]. Therefore, the diffusion of species within the membranes, i.e. $\forall x/(x_c \geq x > x_b)\hat{}(x_a \geq x > x_0)$ can be described by the second Fick's law:

$$\frac{\partial C_i}{\partial t} = D_i \frac{\partial^2 C_i}{\partial x^2} \tag{10}$$

where C_i and D_i are the concentration and the diffusion coefficient of S, M or Q species. The changes on the concentration of H^+ and

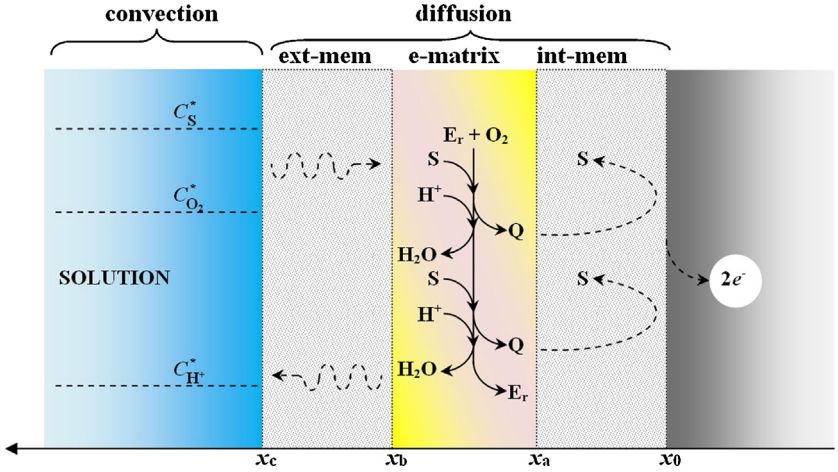

Fig. 1. Scheme of the sandwich-type amperometric biosensor considered for the model.

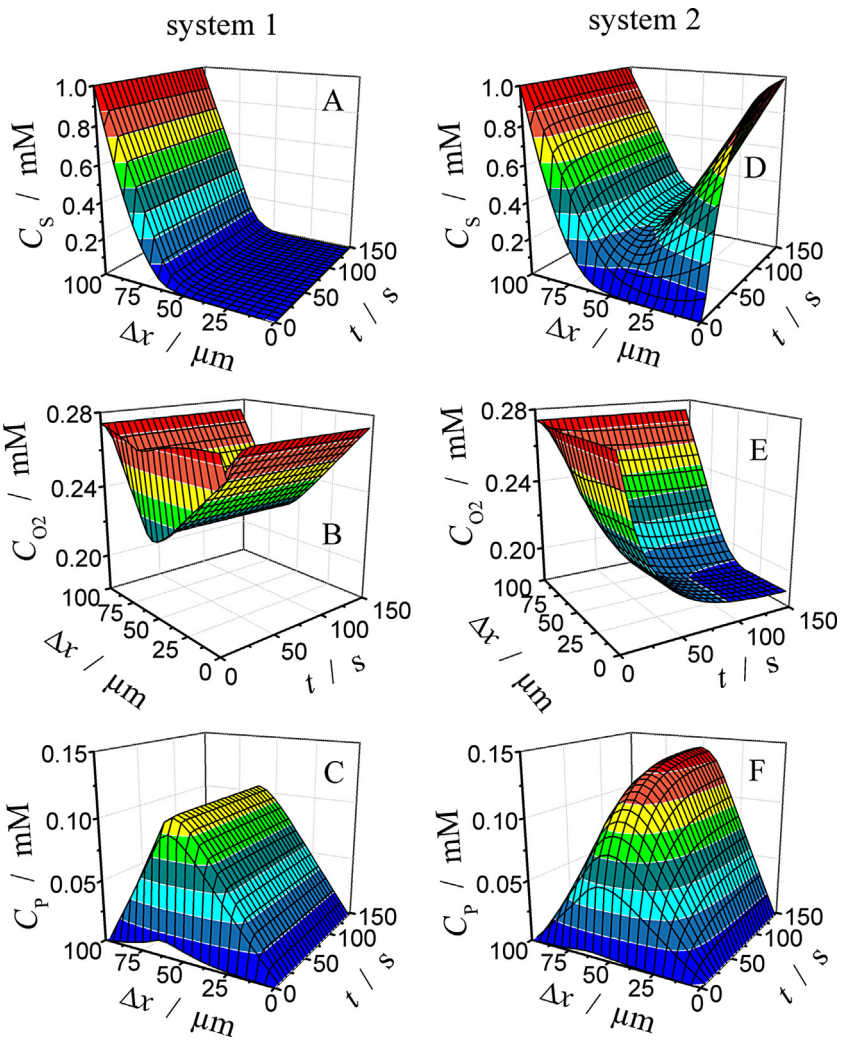

Fig. 2. Theoretical dependence of C_S, C_{O_2} and C_P on time and space when a chronoamperometric biosensor works according to the scheme of system 1 (A–C) and system 2 (D–F). The parameters used are: $C_s^* = 1 \times 10^{-3}$ M, $D_S = 1 \times 10^{-6}$ cm^2 s^{-1}, $D_P = 5 \times 10^{-6}$ cm^2 s^{-1}, $D_M = 1 \times 10^{-5}$ cm^2 s^{-1}, $\Delta x = 100$ μm, $K_S = 10^{-2}$ M, $K_M = 10^{-4}$ M, $v_{max} = 2 \times 10^{-2}$ M s^{-1}, $K_{SM} = 10^{-5}$ M^2.

H_2O are not considered, since it is supposed to work in an aqueous buffered solution. The reactions at the enzymatic matrix are obtained by combining Eq. (8) with the second Fix's law. Thus, $\forall x/(x_b \geq x > x_a)$:

$$\frac{\partial C_i}{\partial t} = D_i \frac{\partial^2 C_i}{\partial x^2} \pm v_i \tag{11}$$

At the electrode surface, the flux of species is described by:

$$\frac{I(t)}{n_e FA} = D_Q \left(\frac{\partial C_Q}{\partial x}\right)_{x=0} = -D_S \left(\frac{\partial C_S}{\partial x}\right)_{x=0} \tag{12}$$

$$\left(\frac{\partial C_M}{\partial x}\right)_{x=0} = 0 \tag{13}$$

Thus, the reduction of quinones gives negative current and the number of electrons (n_e) is 2. Eqs. (10)–(13) can be evaluated by their reformulation into the following finite difference expressions where, for the case of $x/(x_c \geq x > x_b)\hat{}(x_a \geq x > x_0)$:

$$(C_i)_j^{t+1} = (C_i)_j^t + \frac{D_i \delta t}{\delta x^2}\left[(C_i)_{j-1}^t - 2(C_i)_j^t + (C_i)_{j+1}^t\right] \tag{14}$$

While for $x/(x_b \geq x > x_a)$:

$$(C_i)_j^{t+1} = (C_i)_j^t + \frac{D_i \delta t}{\delta x^2}\left[(C_i)_{j-1}^t - 2(C_i)_j^t + (C_i)_{j+1}^t\right] \pm \frac{v_{max}}{\left[1 + K_S/(C_S)_j^t + K_M/(C_M)_j^t + K_{SM}/(C_S C_M)_j^t\right]} \tag{15}$$

The thickness of most real sandwich-type biosensors ($\Delta x = 100\delta x$) goes between 10 and 100 μm [10,11,26,27]. The subscript j corresponds to a given position within the membrane. The sign minus is used to evaluate the concentration profiles of S and M while the sign plus is employed for the product Q. At the electrode surface ($x = 0$):

$$\Psi(\tau) = \frac{I(\tau)}{n_e FAC_S^*}\frac{\delta t}{\delta x} = \frac{D_Q \delta t}{\delta x^2}\frac{(C_Q)_1^t}{C_S^*} \tag{16}$$

In the last expression, $\Psi(\tau)$ corresponds to the dimensionless current at the time $\tau = N\delta t$, D_Q is the diffusion coefficient of the electroactive product Q, and C_S^* is the value of C_S in the bulk, Fig. 1. The dimensionless diffusion coefficient of the mediator ($D_M \delta t/\delta x^2$) was fixed to 0.45 and the dimensioned value of D_M was considered to be 1×10^{-5} cm^2 s^{-1} [10,28]. Calculations performed with Eqs.

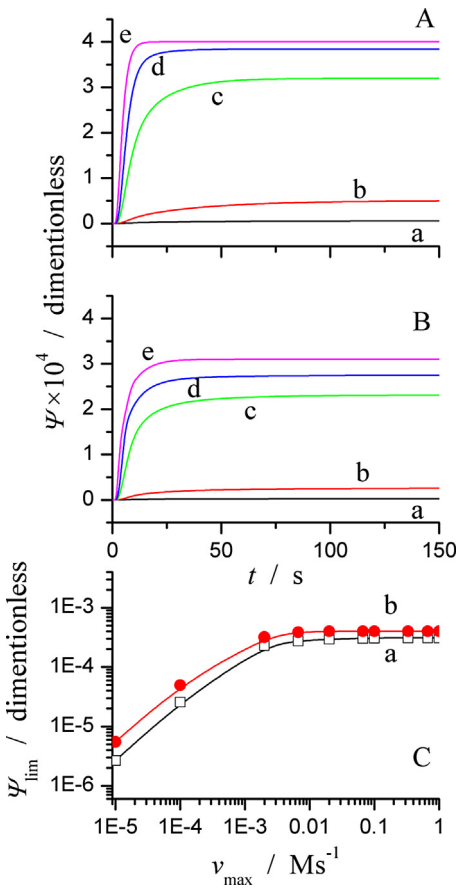

Fig. 3. Chronoamperometric profiles calculated for different values of v_{max} for (A) $C_S = 10^{-3}$ M and (B) $C_S = 10^{-2}$ M according to reaction Scheme 1, v_{max}/M s^{-1} = (a) 10^{-5}, (b) 10^{-4}, (c) 2×10^{-3}, (d) 7×10^{-3}, (e) 1. (C) Theoretical dependence of Ψ_{lim} on v_{max} for C_S/M = (a) 10^{-2}, (b) 10^{-3}. Other parameters are: $D_S = 1 \times 10^{-6}$ cm^2 s^{-1}, $D_P = 5 \times 10^{-6}$ cm^2 s^{-1}, $D_M = 1 \times 10^{-5}$ cm^2 s^{-1}, $K_S = 10^{-2}$, $K_M = 10^{-4}$ M, $\Delta x = 100$ μm.

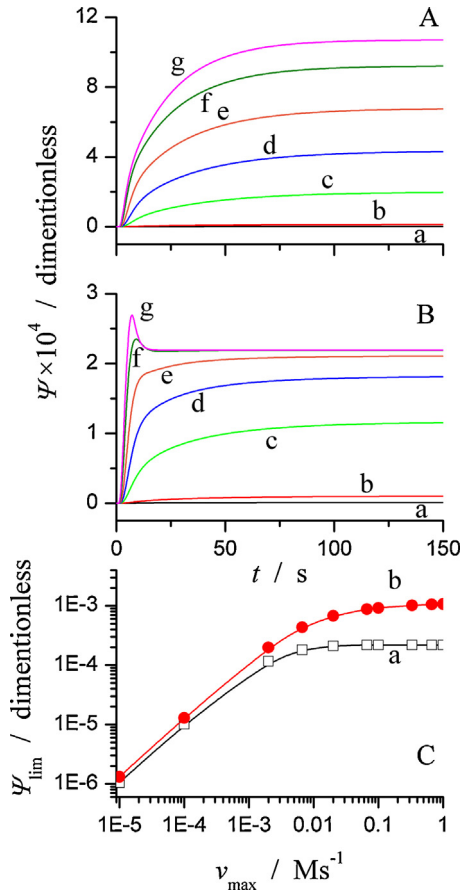

Fig. 4. Chronoamperometric profiles calculated for different values of v_{max} for (A) $C_S = 10^{-3}$ M and (B) $C_S = 10^{-2}$ M according to reaction Scheme 2, v_{max}/M s^{-1} = (a) 10^{-5}, (b) 10^{-4}, (c) 2×10^{-3}, (d) 7×10^{-3}, (e) 0.02, (f) 0.1, (g) 1. (C) Theoretical dependence of Ψ_{lim} on v_{max} for C_S/M = (a) 10^{-2}, (b) 10^{-3}. Other parameters are: $D_S = 1 \times 10^{-6}$ cm^2 s^{-1}, $D_P = 5 \times 10^{-6}$ cm^2 s^{-1}, $D_M = 1 \times 10^{-5}$ cm^2 s^{-1}, $K_S = 10^{-2}$, $K_M = 10^{-4}$ M, $K_{SM} = 10^{-5}$ M^2, $\Delta x = 100$ μm.

(14)–(16) provided the theoretical chronoamperometric transients for this model of PPO sandwich-type biosensors.

3. Results and discussion

The results presented in this manuscript are compared or related to those of a first generation sandwich-type biosensor where an oxidase enzyme follows a ping-pong reaction mechanism [10,11]. The ping-pong reaction scheme corresponds to a simpler system and the respective equations have been included in Appendix A [10].

Fig. 2 compares the dependence of the concentration for substrate (A, D), mediator (B, E) and enzymatic product (C, F) on distance and time. All plots exhibit the evolution of concentration of a given species during a hypothetical chronoamperometric experiment corresponding to a biosensor prepared with an oxidase that follows a ping-pong mechanism (A–C) or with PPO (D–F). The *x*-axes correspond to the thickness of the biosensor and the *t*-axes correspond to the time elapsed after the addition of S to buffer solution. Although kinetic constants and other physicochemical parameters have been kept identical for each system, the comparison of the plots placed in the right and left columns show remarkable differences between both reaction mechanisms. For the analysis of these plots it is necessary to keep in mind that the thickness of the biosensor can be divided into three regions corresponding to the outer membrane, the enzymatic matrix, and the inner membrane.

Let us now focus on the concentration changes of the substrate, Fig. 2A and D. At the external edge of the biosensor the value of C_S is the same than that of the bulk of solution. The value of C_S decreases almost linearly through the outer membrane and it reaches a minimum value in the enzymatic matrix. In both cases the enzyme consumes the substrate but, the situation changes within the inner membrane though. The system 2 has an electrocatalytic reaction that regenerates the substrate at electrode surface, while there is not such reaction in the case of system 1. As a result, C_S remains close to zero within the inner membrane of system 1, but in the case of system 2 the value of C_S increases more or less linearly from the edge at the enzymatic matrix to the electrode surface.

With regards to the concentration changes of the mediator both enzymatic reactions consume the species M, but system 1 generates it back by the electrocatalytic reaction, Fig. 2B and E. This reaction contributes to keep the value of C_M relatively constant within the biosensor. Conversely, system 2 does not have an alternative source of O_2 and the only way to restore M into the enzymatic matrix is by its diffusion from the solution.

Both systems show quite similar concentration profiles for the product of the enzymatic reactions, Fig. 2C and F. In both cases, the maximum value of C_P is observed within the enzymatic matrix and it decreases towards the electrode surface where it is consumed and towards the solution where it is diluted. The main difference between those profiles corresponds to the larger amount of product generated by system 2 with regards to the system 1, which is a consequence of the electrocatalytic generation of S species. The

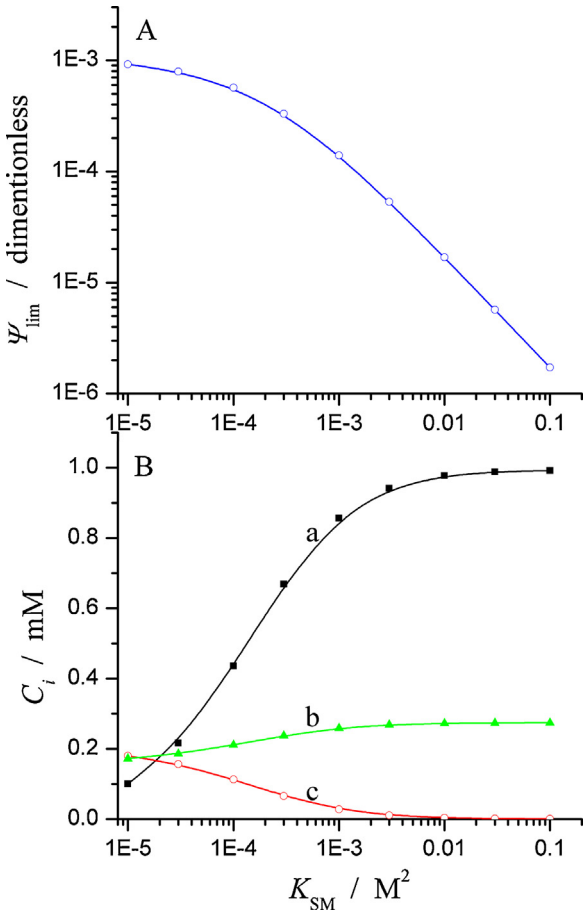

Fig. 5. (A) Theoretical dependence of Ψ_{lim} on K_{SM}. (B) Average values of (a) C_S, (b) C_P and (c) C_M within the enzymatic membrane calculated for different values of K_{SM}, system 2. The parameters used are: $C_s^* = 10^{-3}$ M, $D_S = 1 \times 10^{-6}$ cm^2 s^{-1}, $D_P = 5 \times 10^{-6}$ cm^2 s^{-1}, $D_M = 1 \times 10^{-5}$ cm^2 s^{-1}, $\Delta x = 100$ μm, $K_S = 10^{-2}$ M, $K_M = 10^{-4}$ M, $\nu_{max} = 0.1$ M s^{-1}.

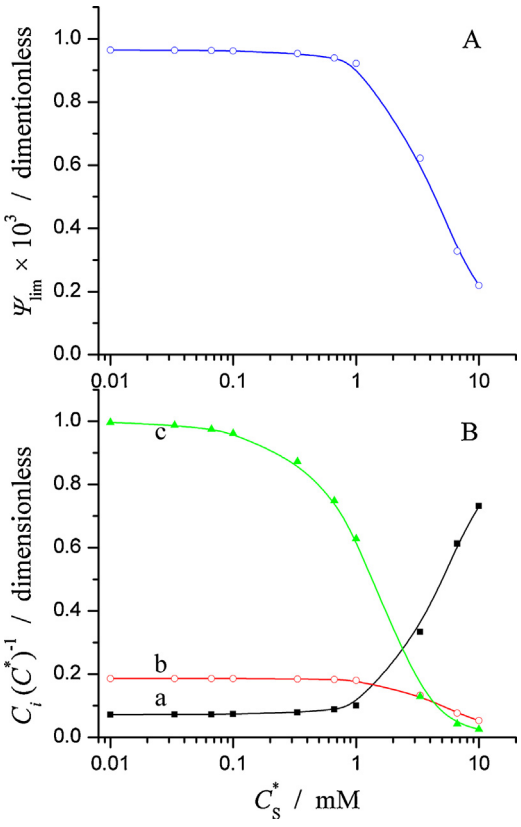

Fig. 6. (A) Theoretical dependence of Ψ_{lim} on C_s^* and (B) of the normalized average values of (a) C_S, (b) C_P and (c) C_M within the enzymatic membrane on C_s^*. The parameters used for system 2 are: $D_S = 1 \times 10^{-6}$ cm^2 s^{-1}, $D_P = 5 \times 10^{-6}$ cm^2 s^{-1}, $D_M = 1 \times 10^{-5}$ cm^2 s^{-1}, $\Delta x = 100$ μm, $K_S = 10^{-2}$ M, $K_M = 10^{-4}$ M, $K_{SM} = 10^{-5}$ M, $\nu_{max} = 0.1$ M s^{-1}.

substrate reaches the enzymatic matrix not only from the solution but also from the electrochemical reaction in the case of system 2. Consequently, an electrocatalytic cycle that enhances the amount of enzymatic product and the respective current stands for this reaction mechanism. In this regard, the product generated by the electrocatalytic reaction affects the steady-state response of the biosensor. This is because the current directly depends on the concentration gradient of the enzymatic product, Eqs. (12) and (16). As a result, a sandwich-type biosensor prepared with an enzyme that reacts according to system 2 would have higher signal of current and longer response time than an equivalent biosensor prepared with an enzyme that reacts according system 1.

Fig. 3A and B shows theoretical chronoamperometric curves corresponding to different values of ν_{max} and considering two different values of C_S for the system 1. The dependence of the limiting dimensionless current Ψ_{lim} on the value of ν_{max} is presented in Fig. 3C. In a previous work it was found that a Ψ_{lim} change linearly with the value of ν_{max} and that Ψ does not depend on the value of C_S [10]. Fig. 3 shows, however, that some changes occur for systems with $C_S > 10^{-3}$ M and $\nu_{max} > 10^{-3}$ M s^{-1}. Provided $C_S < 10^{-3}$ M, theoretical chronoamperometric curves are identical to those presented in Fig. 3A. However, the current will be lower than that expected because the mediator has been depleted into the enzymatic matrix and it is the limiting species of the enzymatic reaction for $C_S > 10^{-3}$, Fig. 3B. Regarding the effect of ν_{max}, it was observed that the limiting current linearly increases with the value of ν_{max} [10]. However, Fig. 3C shows that Ψ_{lim} increases linearly only for $\nu_{max} < 10^{-3}$ M s^{-1}. Above this value, the dependence of Ψ_{lim} on ν_{max} deviates from the expected linear behavior until Ψ_{lim} reaches a plateau for $\nu_{max} > 0.3$ M s^{-1}. A similar behavior can be observed for the system 2, Fig. 4C. In this regard, the deviation from linearity observed in Figs. 3C and 4C can be used to estimate ν_{max} by relating this value with the concentration of enzyme used to prepare a given biosensor. From the comparison of Figs. 3 and 4 it is also possible to observe that the electrocatalytic cycle of system 2 provides higher current than that of system 1 if $C_S \leq 10^{-3}$ M. Nevertheless, if C_S is close to 10^{-2} M or above this value, then $C_M \to 0$ within the enzymatic matrix and the system 2 would show lower values of Ψ_{lim} than system 1, Figs. 3B and 4B. Moreover, chronoamperometric curves of system 2 can show peak-shaped profiles due to the depletion of C_M if the values of ν_{max} and C_S are both as high as in curves Fig. 4B(f and g).

Fig. 5 shows the effect of the parameter K_{SM} on the value of Ψ_{lim} as well as on the average values of C_S, C_P and C_M within the enzymatic matrix. Fig. 5A shows, in a logarithmic scale, that Ψ_{lim} diminishes when the value of K_{SM} is increased. In this regard, the diminution of Ψ_{lim} indicates that less amount of enzymatic product reaches the electrode surface. Chronoamperometric curves calculated for $K_{SM} < 10^{-5}$ M^2 do not change the value of Ψ_{lim}, not shown. The increment of K_{SM} diminishes the value of the last term of Eq. (15) and so, it slows down the velocity of the enzymatic reaction. This effect can be more clearly observed in Fig. 5B, where the concentrations of S and M reach practically the values of the solution bulk for $K_{SM} > 10^{-2}$ M^2. Under these conditions, neither C_S nor C_M would be limiting the enzymatic reaction. On the contrary, both species are in excess while the kinetics of the enzyme is limiting the generation of product.

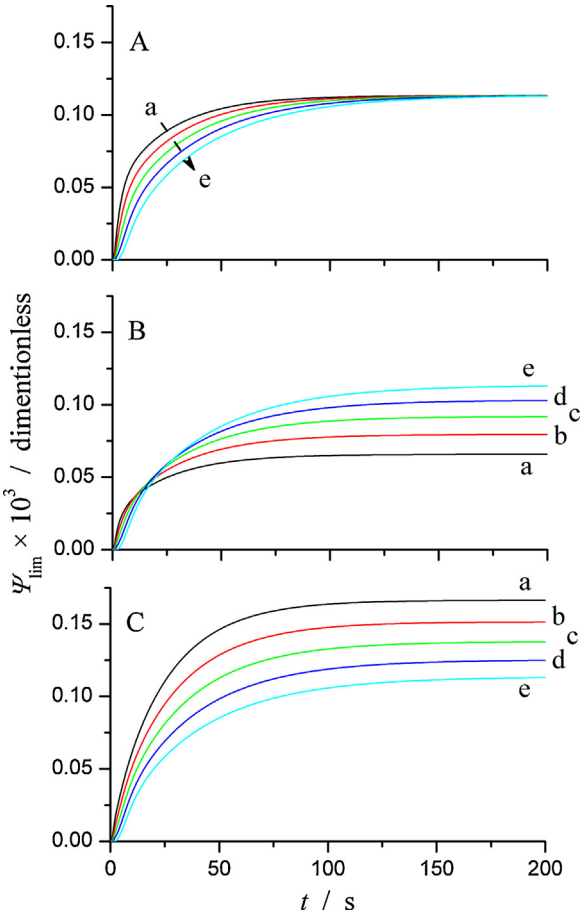

Fig. 7. Chronoamperometric profiles calculated for different thicknesses of (A) outer membrane, (B) enzymatic matrix, and (C) inner membrane. The parameters used for system 2 are: $C_s^* = 10^{-3}$ M, $D_S = 1 \times 10^{-6}$ cm^2 s^{-1}, $D_P = 5 \times 10^{-6}$ cm^2 s^{-1}, $D_M = 1 \times 10^{-5}$ cm^2 s^{-1}, $K_S = 10^{-2}$ M, $K_M = 10^{-4}$ M, $K_{SM} = 10^{-5}$ M, $v_{max} = 10^{-3}$ M s^{-1}. $\Delta x_m/\mu$m = (a) 13, (b) 18, (c) 23, (d) 28, and (e) 33.

Fig. 6A shows the dependence of Ψ_{lim} on the value of C_S^*. The value of Ψ_{lim} is independent of C_S^* for $C_S^* < 10^{-3}$ M. Above this concentration range, the value of Ψ_{lim} diminishes when C_S^* is increased. To explain this behavior the dependence of normalized average values of C_S, C_P and C_M within the enzymatic membrane is analyzed on the value of C_S^*, Fig. 6B. The values of C_S and C_P have been divided by C_S^*, curves (a, b), while for the case of the mediator it has been considered the ratio C_M/C_M^*, curve (c). For solutions with $C_S^* < 10^{-3}$ M the average concentration of S within the enzymatic matrix is approximately constant and its value is close to 7% of C_S^*. The relative amount of S increases within the sensor for $C_S^* > 10^{-3}$ M since the enzymat C_S^* reaction is being limited by the diffusion of M. Accordingly, the normalized concentrations of P and M decrease when the value of C_S^* increases above 10^{-3} M, curves (b and c).

So far the discussion has been focused on diverse aspects related to the enzyme kinetics of different sandwich-type biosensors. Fig. 7 shows changes that can be observed on chronoamperometric responses due to variations of the geometric characteristics of the sensor. Fig. 7A shows the effect of varying the thickness of the outer membrane. All curves have the same value of Ψ_{lim} but their response-time is conditioned by the diffusion of S within this membrane. In other words, the slower response is observed for the sensors with thicker external membrane. The thickness of the enzymatic matrix, however, affects the response-time and the sensitivity of the sensor, Fig. 7B. Even though the highest response of current is expected for sensors prepared with the thickest enzymatic matrix, such sensors would present also the slowest response-time, curve 7B(e). The enzymatic sensors prepared with the thinnest inner membrane should have the highest value of current, while the response-time does not depend on the thickness of this membrane, Fig. 7C. These results are consistent with experimental data corresponding to biosensors prepared with lactate oxidase [11]. The reaction of lactate oxidase can be described according to a ping-pong mechanism such as that described by system 1 [10].

Table 1
Comparison between the variables used in this work and experimental data collected from references.

	Theoretical data used in this work	Experimental data	References
K_{M-M}/mM	10^1 [a]	$10^{-1} \rightarrow 10^2$	[29,30]
k_{cat}/s^{-1}	$10^{-1} \rightarrow 10^4$	$10^0 \rightarrow 10^3$	[29,31]
K_{O2}/μM	10^2	47	[31]
C_E/M	$10^{-9} \rightarrow 10^{-4}$	$10^{-9} \rightarrow 10^{-4}$	[31–33]
V_{max}/Ms^{-1}	$10^{-5} \rightarrow 1$	$10^{-5} \rightarrow 10^{-1}$	
C_S^*/M	$10^{-5} \rightarrow 10^{-2}$	$10^{-9} \rightarrow 10^{-3}$	[2,34–37]
$\Delta x/\mu$m	$80 \rightarrow 100$	$10 \rightarrow 100$	[10,12,26,38]

[a] It is considered that $K_{M-M} = K_S$.

4. Connection between theoretical and experimental parameters

Table 1 compares experimental data with the corresponding theoretical parameters used in this work. Although Michaelis-Menten equation would not be proper for describing PPO biosensors, experimental parameters indicate that such equation would be suitable for the analysis of most PPO biosensors provided $C_M^*(C_S^*)^{-1} > 10$. Under this condition, it can be considered that $K_S \gg [K_M (C_M)^{-1} + K_{SM} (C_S C_M)^{-1}]C_S$, and so the Michaelis–Menten constant (K_{M-M}) tends to K_S. The upper limit of V_{max} was estimated from the product between the maximum values of k_{cat} and C_E, while the theoretical data of k_{cat} and C_E have been calculated from the set of values considered for V_{max}. With regards to the thickness, most sandwich-type biosensors have rather high values of this parameter since it depends on the width of the diffusional membranes employed for the sensor. The diverse values informed for K_{M-M}, k_{cat}, and V_{max}, result from the large number of enzymes corresponding to the family of PPOs.

5. Conclusions

A numerical model for the description of sandwich-type amperometric biosensors containing PPO as the recognition catalytic element has been presented. The reaction mechanism of PPO was analyzed according to Fromm's method to get an expression that considers the enzyme kinetics of this kind of enzymes. Chronoamperometric profiles of biosensors prepared with an oxidase enzyme such as GOX (system 1) and with PPO (system 2) are compared. Although both systems consume oxygen as mediator of the enzymatic reaction, the electrochemical step of system 1 can regenerate it back from H_2O_2, while this is not possible in the case of system 2 since PPO produces H_2O and quinone species.

The concentration of reagents and products within the enzymatic matrix rarely has the same value than the bulk. Those values are the result of diverse parameters such as the concentration and diffusion coefficients of involved species, the enzymatic constants, and the dimensions of the biosensor that determine the results of Eqs. (14)–(16). The thickness of membranes has noticeable influence on the response of the sensor. The outer membrane affects the response-time of the sensor, while the inner membrane influences the amplitude of the signal. With regards to the enzymatic matrix, there is a committed relationship for its thickness since

the thinnest matrixes provides the fastest responses as well as the lowest values of current.

Appendix A. Supplementary data

Supplementary data associated with this article can be found, in the online version, at http://dx.doi.org/10.1016/j.snb.2014.10.105.

References

[1] P.T. Kissinger, Biosensors – a perspective, Biosensors and Bioelectronics 20 (2005) 2512–2516.
[2] B. Serra, Á.J. Reviejo, J.M. Pingarrón, Application of electrochemical enzyme biosensors for food quality control, in: S. Alegret, A. Merkoçi (Eds.), Comprehensive Analytical Chemistry, Elsevier B.V., 2007, pp. 255–298 (Chapter 13).
[3] M. Campàs, J.L. Marty, Amperometric enzyme sensors for the detection of cyanobacterial toxins in environmental samples, in: S. Alegret, A. Merkoçi (Eds.), Comprehensive Analytical Chemistry, Elsevier B.V., 2007, pp. 331–355 (Chapter 16).
[4] J. Wang, Electrochemical glucose biosensors, Chemical Reviews 108 (2008) 814–825.
[5] V. Scognamiglio, Nanotechnology in glucose monitoring: advances and challenges in the last 10 years, Biosensors and Bioelectronics 47 (2013) 12–25.
[6] J.I. Njagi, S.M. Kagwanja, The Interface in Biosensing: Improving Selectivity and Sensitivity, Interfaces and Interphases in Analytical Chemistry, American Chemical Society, 2011, pp. 225–247.
[7] F.S. Ligler, Perspective on optical biosensors and integrated sensor systems, Analytical Chemistry 81 (2009) 519–526.
[8] Zhao Yue, Fred Lisdat, Wolfgang J. Parak, Stephen G. Hickey, Liping Tu, Nadeem Sabir, Dirk Dorfs, Nadja C. Bigall, Quantum-dot-based photoelectrochemical sensors for chemical and biological detection, Applied Materials & Interfaces 5 (2013) 2800–2814.
[9] M. Fernández-Fernández, M.A. Sanromán, D. Moldes, Recent developments and applications of immobilized laccase, Biotechnology Advances 31 (2013) 1808–1825.
[10] M.R. Romero, A.M. Baruzzi, F. Garay, Mathematical modeling and experimental results of a sandwich-type amperometric biosensor, Sensors and Actuators B 162 (2012) 284–291.
[11] M.R. Romero, A.M. Baruzzi, F. Garay, How low does the oxygen concentration go within a sandwich-type amperometric biosensor? Sensors and Actuators B 174 (2012) 279–284.
[12] J.C. Espín, P.A. García-Ruiz, J. Tudela, R. Varón, F. García-Cánovas, Monophenolase and diphenolase reaction mechanisms of apple and pear polyphenol oxidases, Journal of Agricultural and Food Chemistry 46 (1998) 2968–2975.
[13] H. Li, R. Luo, Modeling and characterization of glucose-sensitive hydrogel: effect of Young's modulus, Biosensors and Bioelectronics 24 (2009) 3630–3636.
[14] B. Csóka, B. Kovács, G. Nagy, Investigation of concentration profiles inside operating biocatalytic sensors with scanning electrochemical microscopy (SECM), Biosensors and Bioelectronics 18 (2003) 141–149.
[15] P.N. Bartlett, K.F.E. Pratt, A study of the kinetics of the reaction between ferrocene monocarboxylic acid and glucose oxidase using the rotating-disc electrode, Journal of Electroanalytical Chemistry 397 (1995) 53–60.
[16] B. Wang, J. Zheng, Y. He, Q. Sheng, A sandwich-type phenolic biosensor based on tyrosinase embedding into single-wall carbon nanotubes and polyaniline nanocomposites, Sensors and Actuators B 186 (2013) 417–422.
[17] C. Apetrei, M.L. Rodríguez-Méndez, J.A. De Saja, Amperometric tyrosinase based biosensor using an electropolymerized phosphate-doped polypyrrole film as an immobilization support. Application for detection of phenolic compounds, Electrochimica Acta 56 (2011) 8919–8925.
[18] W. Song, D.-W. Li, Y.-T. Li, Yang Li, Yi-Tao Long, Disposable biosensor based on graphene oxide conjugated with tyrosinase assembled gold nanoparticles, Biosensors and Bioelectronics 26 (2011) 3181–3186.
[19] F. Campanhã Vicentini, B.C. Janegitz, C.M.A. Brett, O. Fatibello-Filho, Tyrosinase biosensor based on a glassy carbon electrode modified with multi-walled carbon nanotubes and 1-butyl-3-methylimidazolium chloride within a dihexadecylphosphate film, Sensors and Actuators B 188 (2013) 1101–1108.
[20] A. Mattevi, To be or not to be an oxidase: challenging the oxygen reactivity of flavoenzymes, Trends in Biochemical Sciences 31 (2006) 276–283.
[21] L. Coche-Guérente, V. Desprez, J.-P. Diard, P. Labbé, Amplification of amperometric biosensor responses by electrochemical substrate recycling. Part I. Theoretical treatment of the catechol–polyphenol oxidase system, Journal of Electroanalytical Chemistry 470 (1999) 53–60.
[22] L. Coche-Guérente, V. Desprez, P. Labbé, S. Therias, Amplification of amperometric biosensor responses by electrochemical substrate recycling: part II. Experimental study of the catechol–polyphenol oxidase system immobilized in a laponite clay matrix, Journal of Electroanalytical Chemistry 470 (1999) 61–69.
[23] D.L. Purich, Initial-rate kinetics of multi-substrate enzyme-catalyzed reactions, in: D.L. Purich (Ed.), Enzyme Kinetics: Catalysis & Control, Elsevier Inc., 2010, pp. 341–343 (Chapter 6).
[24] F. Garay, C.A. Barbero, Charge neutralization process of mobile species at any distance from the electrode/solution interface. 1. Theory and simulation of concentration and concentration gradients developed during potentiostatic conditions, Analytical Chemistry 78 (2006) 6733–6739.
[25] F. Garay, C.A. Barbero, Charge neutralization process of mobile species developed during potentiodynamic conditions. Part 1: theory, Journal of Electroanalytical Chemistry 624 (2008) 218–227.
[26] I. Iliev, P. Atanasov, S. Gamburzev, A. Kaisheva, V. Tonchev, Transient response of electrochemical biosensors with asymmetrical sandwich membranes, Sensor and Actuators B 8 (1992) 65–72.
[27] A.A. Aziz, Mathematical modeling of an amperometric glucose sensor: the effect of membrane permeability and selectivity on performance, Jurnal Teknologi 51 (2009) 77–94.
[28] M. Jamnongwong, K. Loubiere, N. Dietrich, G. Hébrard, Experimental study of oxygen diffusion coefficients in clean water containing salt, glucose or surfactant: consequences on the liquid-side mass transfer coefficients, Chemical Engineering Journal 165 (2010) 758–768.
[29] http://www.brenda-enzymes.org/enzyme.php?ecno=1.10.3.1
[30] https://www.sigmaaldrich.com/content/dam/sigma-aldrich/docs/Sigma/Datasheet/8/t3824dat.pdf
[31] L.G. Fenoll, J.N. Rodríguez-López, F. García-Sevilla, P.A. García-Ruiz, R. Varón, F. García-Cánovas, J. Tudela, Analysis and interpretation of the action mechanism of mushroom tyrosinase on monophenols and diphenols generating highly unstable o-quinones, Biochimica et Biophysica Acta 1548 (2001) 1–22.
[32] Y. Matoba, T. Kumagai, A. Yamamoto, H. Yoshitsu, M. Sugiyama, Crystallographic evidence that the dinuclear copper center of tyrosinase is flexible during catalysis, The Journal of Biological Chemistry 281 (2006) 8981–8990.
[33] F. Zekiri, A. Bijelic, C. Molitor, A. Rompel, Crystallization and preliminary X-ray crystallographic analysis of polyphenol oxidase from Juglans regia (jrPPO1), Acta Crystallographica F70 (2014) 832–834.
[34] S. Cosnier, J.J. Fombon, P. Labbe, D. Limosin, Development of a PPO-poly(amphiphilic pyrrole) electrode for onsite monitoring of phenol in aqueous effluents, Sensors and Actuators B 59 (1999) 134–139.
[35] E. Han, D. Shan, H. Xue, S. Cosnier, Hybrid material based on chitosan and layered double hydroxides: characterization and application to the design of amperometric phenol biosensor, Biomacromolecules 8 (2007) 971–975.
[36] J. Abdullah, M. Ahmad, L.Y. Heng, N. Karuppiah, H. Sidek, An optical biosensor based on immobilization of laccase and MBTH in stacked films for the detection of catechol, Sensors 7 (2007) 2238–2250.
[37] F. Vianello, S. Ragusa, M.T. Cambria, A. Rigo, A high sensitivity amperometric biosensor using laccase as biorecognition element, Biosensors and Bioelectronics 21 (2006) 2155–2160.
[38] J. Shim, J.J. Woo, S.H. Moon, G.Y. Kim, A preparation of a single-layered enzyme-membrane using asymmetric pBPPO base film for development of pesticide detecting biosensor, Journal of Membrane Science 330 (2009) 341–348.

Biography

Fernando Sebastián Garay, Doctor (Universidad Nacional de Córdoba, 2002). Currently he is adjunct professor at the Department of Physical Chemistry, School of Chemical Science, Universidad Nacional de Córdoba and Research Fellow of CONICET, Argentina. His fields of interest include electrochemistry, numerical and digital simulations, analytical chemistry, in situ techniques, polymer science and biosensors.